Applied Energy 378 (2025) 124737

Contents lists available at ScienceDirect

Applied Energy

journal homepage: www.elsevier.com/locate/apenergy

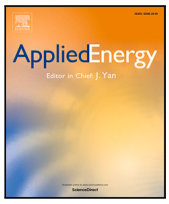

Enhancing grid stability in PV systems: A novel ramp rate control method utilizing PV cooling technology

Koki Iwabuchi [a,*], Daichi Watari [a], Dafang Zhao [a], Ittetsu Taniguchi [a], Francky Catthoor [b,c], Takao Onoye [a]

[a] Graduate School of Information Science and Technology, Osaka University, 1-5 Yamada-oka, Suita, 5650871, Osaka, Japan
[b] imec, Kapeldeef 75, Heverlee, 3001, Belgium
[c] ESAT, KULeuven, Kasteelpark Arenberg 10, Heverlee, 3001, Belgium

ARTICLE INFO

Keywords:
PV systems
Power grids
Power ramp rate control
PV cooling

ABSTRACT

Rapid fluctuations in solar irradiation lead to significant variability in PV power output. Traditional ramp rate control methods use battery energy storage systems to smooth power outputs and provide a more consistent supply to the grid. However, these methods require high initial costs and substantial maintenance. In this study, we propose a novel method for controlling PV power output ramp rates using cooling technology, which is essential to stabilize grid operations and ancillary services. The proposed method adjusts power generation efficiency in real-time by controlling PV panel temperature, leveraging their thermoelectric properties. The effectiveness of our method was validated by simulation based on real-world data, which showed reductions in mean and maximum ramp rates of 43.5% and 76.2%, respectively, compared to traditional battery storage solutions. Notably, these improvements were achieved with a cooling unit having a coefficient of performance of less than 10 and a minimal battery capacity of 20 kWh, highlighting the efficiency of the method and its potential to significantly lower system costs and environmental impacts compared to traditional control strategies.

1. Introduction

Solar energy is one of the most promising renewable energy alternatives to fossil fuels for mitigating global warming. As photovoltaic (PV) generation is increasingly adopted, it poses challenges to the operation of the power grid. PV generation depends on temperature, solar irradiation intensity, and other weather factors. In particular, solar irradiation, which is converted to electricity by solar cells, varies instantaneously and significantly with different locations and weather conditions. This can result in high power output ramp rates and grid frequency issues, which can create grid stability concerns. Various methods have been studied so far to solve this problem.

Three main methods have been studied so far as a way to reduce short-term power fluctuations in PV power generation. The first is to combine PV power generation with some form of battery energy storage system (BESS) [1]. While BESS has the advantage of large capacity and the ability to handle large ramp rates, they have the disadvantage of high installation and maintenance costs and a large environmental impact. The second method is to use controllable power generation by fuel, such as gas turbines [2]. Although fuel-based power generation has the advantage of rapid mass power generation, it has the disadvantages of high system costs and a large environmental impact, as does a large-capacity battery. The third is the use of dump loads to reduce the power input to the grid during periods of high variability [3]. A dump load consists of a resistor and a controller that controls the power flowing to the load. Consuming or limiting power through dump loads has the advantage of very low system cost, but dumped power cannot be reused. These methods have the disadvantages of high system cost and environmental impact or ineffective use of power. Our proposed method controls the ramp rate by adjusting the PV generation itself, without using a large-capacity battery, gas turbine, or dump load. Therefore, unlike previous studies, the system costs and environmental impact are low, and the power can be used effectively.

In the proposed method, the dependence of PV power generation efficiency on the temperature of the PV panel is focused, allowing the adjustment of the PV power generation itself. At high temperatures, the carrier concentration at the p–n junction of the PV module increases, resulting in lower module efficiency [4]. Previous studies on PV cooling exist [5], but they were aimed at increasing the efficiency of PV power generation and not at controlling the ramp rate.

* Corresponding author.
E-mail addresses: iwabuchi.koki@ist.osaka-u.ac.jp (K. Iwabuchi), watari.daichi@ist.osaka-u.ac.jp (D. Watari), zhao.dafang@ist.osaka-u.ac.jp (D. Zhao), i-tanigu@ist.osaka-u.ac.jp (I. Taniguchi), Francky.Catthoor@imec.be (F. Catthoor), onoye@ist.osaka-u.ac.jp (T. Onoye).

https://doi.org/10.1016/j.apenergy.2024.124737
Received 4 January 2024; Received in revised form 2 September 2024; Accepted 15 October 2024
Available online 1 November 2024

In this paper, we propose a ramp rate control method to mitigate the Eyield fluctuations of a specific PV plant or installation by adjusting that plant's PV generation using onsite PV cooling. In the proposed method, energy management of PV system including PV cooling units is carried out based on power demand, weather information and PV generation forecast in microgrid. The proposed method has a low system cost and environmental impact because it does not require the operation of a gas turbine or a large-capacity battery. Also, the power saved during output power fluctuations is not dumped, but effectively utilized in the PV cooling unit. The main contributions and Novelty of this work are shown below:

- **Effective ramp rate reduction**: Our proposed method significantly reduces the mean ramp rate by 43.5% and the maximum ramp rate by 76.2% compared to the battery-only method. This substantial improvement underscores our method's effectiveness in stabilizing PV output and mitigating grid fluctuations.
- **Cost and environmental impact**: By avoiding the use of gas turbines and high-capacity batteries, our approach not only minimizes operational costs but also further reduces the environmental footprint of managing PV system variability.

This paper is structured as follows. First, related research is presented separately for ramp rate control methods and PV cooling methods in Section 2. Second, an overview of the proposed ramp rate control method using PV cooling is presented in Section 3. Section 4 describes the introduced system model in detail and presents the mathematical formulation of the PV system operation optimization problem, including the PV cooling unit. Finally, simulations demonstrate the effectiveness of the proposed method in Section 5 and summarize it in Section 6.

2. Related works

Related research on ramp rate control is presented, broadly classified into three categories: those using battery energy storage system (BESS), those using fuel-based power generation, and those using power consumption or limitation by dump loads. Related research on PV cooling is also presented at the end of this section.

2.1. Ramp rate control methods

The use of BESS is the most well-studied approach. A detailed BESS sizing methodology was presented that evaluates aspects of energy requirements, power, and discharge rate [1]. The case study was evaluated using mission profiles of solar irradiation and ambient temperature for one year in Goiânia (Brazil). The sizing approach reduced the BESS volume by 57.14% compared to previous BESS designs in the literature. With respect to BESS sizing, it is also known that the solar irradiation profile has a significant impact on the power and energy requirements of the BESS [6]. It was found that BESS power rating of 60% of the nominal power of the PV string is sufficient to smooth almost all detected PV power ramps, even with strict ramp-rate limits. For methods using BESS, ramp rate control that also takes battery degradation into account is important. The commonly used algorithms were compared, especially in terms of battery status, which is directly related to battery life performance [7]. In that comparison, BESS capacity required for each algorithm was also analyzed. Through the comparison, the control algorithm with the second-order low-pass filter not only used less battery capacity than the other algorithms, but also had fewer cycles and reduced magnitude of charge change, and thus was expected to have a longer lifetime. With respect to battery degradations, the importance of battery operating temperature and the effect of battery size and degree of ramp rate limitation on battery degradation are also highlighted [8]. In the hybrid energy storage and management system for battery and hydrogen storage, the model predictive control strategy was used to manage the degradation of the energy storage system, thereby extending the life of the system [9]. The algorithm, with three basic goals of reduced battery cycles, minimal energy storage requirements, and ramp rate violation-free operation, extended expected battery life and cost-effective smoothing [10]. The smoothing quality of PV output with the help of BESS was investigated using several approaches, including low-pass filtering, moving average filtering, Gaussian filtering, and Saviztky–Golay filtering [11]. The performance of moving average and low-pass filters is relatively unacceptable, especially when long window sizes and time constants are used, which in turn degrade the performance of BESS. In contrast, using the Savitzky–Golay filter was shown to reduce the battery ramp rate and battery charge/discharge power while smoothing out solar power fluctuations. For facilities consisting of PV system and BESS, fluctuations were smoothed out while taking into account the state of charge (SOC) [12]. The approach consists of two algorithms: moving average control, which uses a fixed window size to estimate a smooth power curve; and SOC control, which aims to provide storage flexibility and SOC close to a reference value. Simulations demonstrated the effectiveness of this approach and its suitability for mitigating the impact of integrating PV into the distribution grid. The ramp rate of the renewable energy power plant was controlled by BESS, a combination of batteries and capacitors [13]. Hybrid solutions with batteries and ultracapacitors may be less expensive than systems consisting solely of batteries, although this depends primarily on the cost and lifetime characteristics of the different technologies. The main cost saving factor is the reduction in unused storage capacity of the battery, which is needed only to avoid exceeding the charge rate limit during short periods of rapid power fluctuations. Besides ultracapacitors, a hybrid energy storage system of supercapacitors and batteries was used to smooth PV power [14]. The results of the experiments show a reduction in the operation of supercapacitors compared to other power smoothing methods when using the new smoothing technique. Similarly, two power smoothing algorithms, the ramp rate method and the moving average method, were compared using a hybrid energy storage system consisting of a supercapacitor and a lithium-ion battery [15]. The experimental results indicate that applying the ramp rate method results in the supercapacitor operating fewer cycles compared to the moving average method. This outcome remained consistent even when altering the capacity of renewable energy sources. Market participation with BESS was examined [16]. A two-layer model predictive control framework for managing wind-solar microgrids, encompassing both islanded and grid-connected modes, has been introduced. The framework is unique in that it integrates two hierarchical control layers, high-layer control and low-layer control, tailored to optimize BESS management and market participation. BESS, as in these studies, is useful in reducing PV output variability. In particular, a large-capacity battery can handle large ramp rate changes. However, not only are system costs, such as equipment and maintenance costs, high, but also the environmental impact is high.

Another means of mitigating the unstable effects of power fluctuations is to use controllable power generation, such as gas turbines. To compensate for the intermittent nature of solar power, the focus was on compressed air injection for fast response of on-demand power generation systems with gas turbines [2]. It was noted that the increased use of renewables and more stringent grid requirements require higher ramp rates for backup power sources, such as gas turbines. Quasi-power simulations conducted using the constant mass flow method showed that, regardless of the starting load, each 2% injection of compressor outlet air flow at ramp up improves the ramp up rate of a large gas turbine by an average of 10%. However, it is still estimated that more than 1 million liters of fuel are consumed annually. The use of gas turbines has the advantage of easy control of the amount of electricity generated. However, like large-capacity batteries, they have the disadvantage of high system costs and environmental impact.

Power suppression with dump loads has proven to be a better option when larger power fluctuations are allowed, with less revenue loss

Table 1
Pros and cons of typical ramp rate control methods.

Ramp rate control methods	Pros	Cons
Battery energy storage systems (BESS)	• The larger the capacity of the battery, the better it can handle large ramp rate changes. • Ability to respond to both sudden increases and sudden decreases in PV power output. • Reduced excess power can be reused.	• The larger the capacity of the battery, the higher the equipment cost, maintenance cost. • The larger the capacity of the battery, the higher the environmental impact. • Quickly degrades with repeated rapid charging and discharging.
Power generation from fuels	• Easy to generate large amounts of power quickly.	• High equipment and maintenance costs. • High environmental impact. • Inability to cope with rapid increases in PV generation output.
Power consumption or limitation by dump loads	• Much lower equipment and maintenance costs.	• Reduced power cannot be reused. • Inability to cope with rapid decreases in PV generation output.

than the use of BESS [3]. The use of dump load controllers has been demonstrated to effectively reduce flicker when clouds pass over PV panels [17]. The use of dump load and the maximum power point tracking control method are highly reliable, but they are not recommended for mitigating PV power fluctuations in large PV plants despite their relatively low cost [18]. This is because they limit the revenue of the owners. However, they can be applied to relatively smaller PV installations at the residential or community level. Furthermore, droop excess power curtailment control is employed to limit the PV output from the inverter, maintaining the voltage within a specified range [19]. This droop excess power curtailment control is based on the relationship between the system frequency and the excess power of the generators. However, in these studies involving power consumption and control through methods such as dump loads and the maximum power point tracking control, the reduced power cannot be reused. Table 1 summarizes the advantages and disadvantages of these three main ramp rate control methods.

2.2. PV cooling methods

Various methods of cooling PV have been studied. Cooling technologies using phase change materials (PCM), nanofluids, and their combination were investigated, and it was found that a passive cooling approach using PCM can improve PV efficiency by up to 20% [5]. The focus was on PCM models used for natural convection and numerical simulations [20]. The use of PCM for thermal energy storage consistently demonstrates a reduction in energy consumption, with potential advantages of up to 20%, especially during peak hours. Sheep fat was used as a new PCM [21]. The results showed that sheep fat cools the PV module more efficiently than paraffin wax, which was used as the conventional PCM. A passive cooling system using natural coolant circulation was proposed [22]. The water flow is a result of buoyancy and gravity. A composite of coconut oil and sunflower oil was used as the PCM. Experimental results showed that the cooling system using coconut oil and sunflower oil as PCM significantly increased the efficiency of the PV panels. Static water, but not flowing water, was also used for cooling with PCM [23]. The latent heat of melting of the PCM and the latent heat of evaporation of the water are used to achieve effective cooling in a passive approach. The daily output was found to be 8.12% and 9.39% higher than that of the PV panel without cooling over the two observed days, respectively. Shape-stabilized PCMs with high energy storage capacity and rapid charge–discharge rates are also under investigation [24]. The facile approach to synthesize novel salt hydrate-based shape-stabilized PCMs by incorporating functionalized graphene nanoplatelets was demonstrated. The addition of graphene nanosheets significantly improved the solar absorption characteristics of pure PCM and simultaneously provided a high photothermal efficiency of 92.6%. Nanofluids are used as coolants and optical filters [25]. The use of nanofluids in PV-thermal systems was found to improve PV efficiency by over 60%, while integration with PCM was found to improve PV-thermal system efficiency by 32%. The effectiveness of nanoparticles was also demonstrated [26]. Three different PV-thermal air collectors were designed, manufactured, and experimentally analyzed. These collectors included the conventional PV-thermal, PV-thermal with a paraffin-based thermal energy storage unit, and PV-thermal with a nano-enhanced paraffin-based thermal energy storage unit. The experimental results indicated a significant improvement in the electrical and thermal performance of the PV-thermal system by utilizing the nano-enhanced thermal energy storage system and increasing the flow rate. However, the high cost of developing nanofluids and nano-PCMs is a key issue in implementing this technology [25]. In addition, the stability of nanomaterials is a concern. It was shown that the “waste heat” from solar cells can be used for desalination to simultaneously produce fresh water and electricity [27]. High and stable freshwater production rates and reduced solar cell temperatures were demonstrated using a five-stage PV-membrane distillation-evaporative crystallizer. This decrease in solar cell temperature resulted in an 8% increase in power generation. The fin plate geometry used on the back of the PV module was a focus of attention [28]. The need for an effective passive cooling strategy in compact PV modules was addressed by considering three different fin geometries (pin fins, Y-shaped fins, and spring fins) using both numerical simulations and experiments. Cooling by PCM, thermoelectric, and aluminum fins was tested [29]. It was observed that while PV with fin systems produced the highest power, PCM, if not properly selected, had an insulating function within the PV panel, increasing the temperature of the panel and reducing its output. An adsorption atmospheric condenser was used as an effective cooling system [30]. This PV panel cooling system provides an average cooling power of 295 W m^{-2} and lowers the temperature of PV panels by at least 10 °C under 1.0 kW m^{-2} solar irradiation. In outdoor field tests, commercial PV panels increased power generation by 13 to 19%. Another advantage of the atmospheric water-based PV panel cooling strategy is that there are few geographic constraints in its application. Active water cooling is the simplest and most effective cooling technique and has been actively studied [31]. However, active water cooling is often impractical. Valuable active water cooling requires an environment with a stable supply of cooling water, and the cooling array must be large enough to offset energy consumption. All PV cooling technologies presented in this section are intended to maximize PV power generation. The subject of our study, the control of power generation by PV cooling, is completely out of scope.

3. Ramp rate control method utilizing PV cooling

This section provides an overview of the proposed ramp rate control method and the use of PV cooling, which is a key concept of the proposed method, along with the target microgrid shown in Fig. 1. The microgrid is a structure that can be connected to or separated from the main grid via a breaker. A microgrid is a local energy community

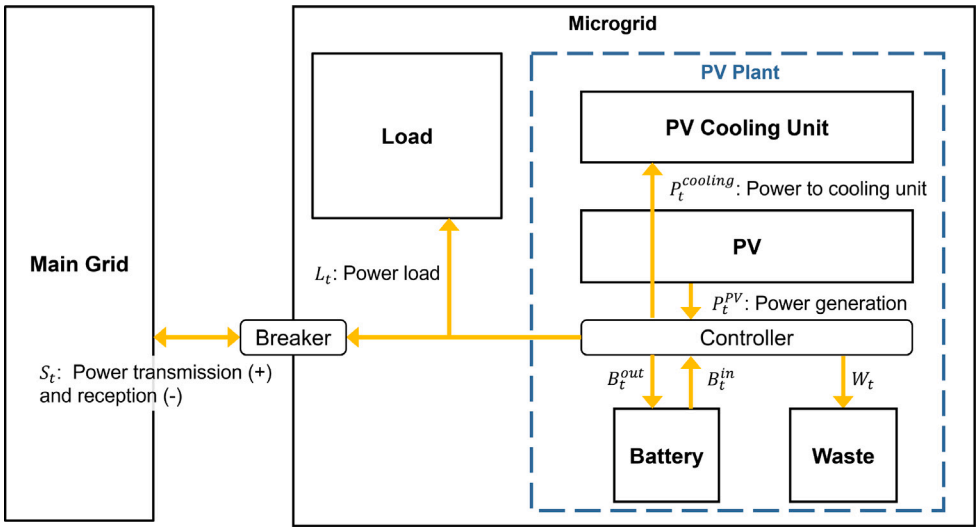

Fig. 1. Targeted microgrid structure with mathematical symbol of each variable.

consisting of energy supply sources and consumption facilities. Fig. 1 shows a schematic of our microgrid model. The microgrid is largely divided into a PV plant and load, which is the power consumption facility. The main components of a PV plant are PV panels, PV cooling units, and batteries. A controller in the PV plant manages the power flow throughout the PV plant based on the power balance and system state. This controller monitors only the power gradient of the PV plant, not the entire grid. The microgrid receives power from the main grid in the event of a power shortage. Whenever possible, excess power is either transmitted to the main grid or consumed by the PV cooling units or batteries, but depending on the ramp rate, it may be wasted within the power plant.

We also note that our proposed ramp rate control method is modular and scalable, as it is designed to be applied at the subsystem level rather than to the PV system as a whole. The PV cooling scheme and associated battery bank are inherently scalable and designed to start with a minimum number of units. Such a decentralized approach does not require centralized cooling efforts. Once the unit design is established, it can be replicated as needed to scale up to full-scale power plant capacity. It is emphasized that the cooling unit performance and battery size used in this study is intentionally modest and is a good candidate for unit size for scalable applications. With this design approach, the method can be easily adapted to PV installations of various sizes and configurations.

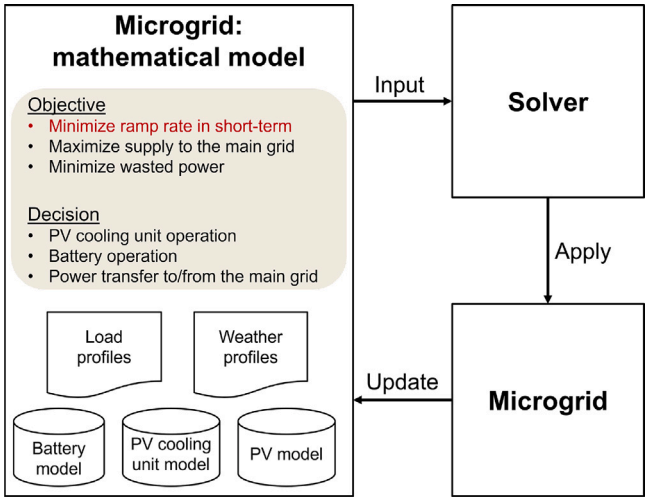

Fig. 2. Overview of the proposed method: Optimization for PV systems, including PV cooling units.

3.1. Overview of the proposed ramp rate control method

An overview of the proposed framework is shown in Fig. 2. The main objective is to minimize short-term PV output ramp rates, e.g., due to transient clouds. The inputs to the method are power load information and weather data. The weather data includes temperature and solar irradiation. The output is a plan that includes PV cooling unit operation, battery operation, and power transfer to and from the main grid. The method performs a process of computing the optimal solution that minimizes a given objective for a finite time horizon. Our strategy involves a detailed operational plan for cooling units and batteries, taking into account both power surplus and demand shortage scenarios at the subsystem level, where the PV plant is connected. This is achieved by dynamically adjusting the cooling operation based on real-time power generation and load data, facilitating both power injection and withdrawal to and from the grid without compromising grid stability.

The main process of the proposed method is as follows. First, load and weather data for a period of time when PV output fluctuations may occur, such as 15 min, are obtained. The PV model is used to obtain PV forecast data on power generation and panel temperature from that weather data. Then optimize energy use, primarily to minimize ramp rates. While it would be possible to minimize ramp rates by reducing power distribution or dumping power, this is undesirable, so maximizing power to the grid and minimizing power dumping are also included in the objectives. Energy use includes operation of PV cooling units and batteries, as well as power transfer to and from the grid. This optimization problem is formulated mathematically, and optimal results can be obtained by a mathematical solver. Finally, the obtained plan is applied to the system operation. The results applied are reflected in the mathematical model.

Our proposed method is designed to operate online by formulating the problem as a mathematical optimization problem in this way. This approach is essential for its functionality, as it enables real-time adjustments based on immediate weather data and PV output forecasts. Our system aims to operate efficiently on cost-effective and widely available hardware platforms such as the Raspberry Pi.

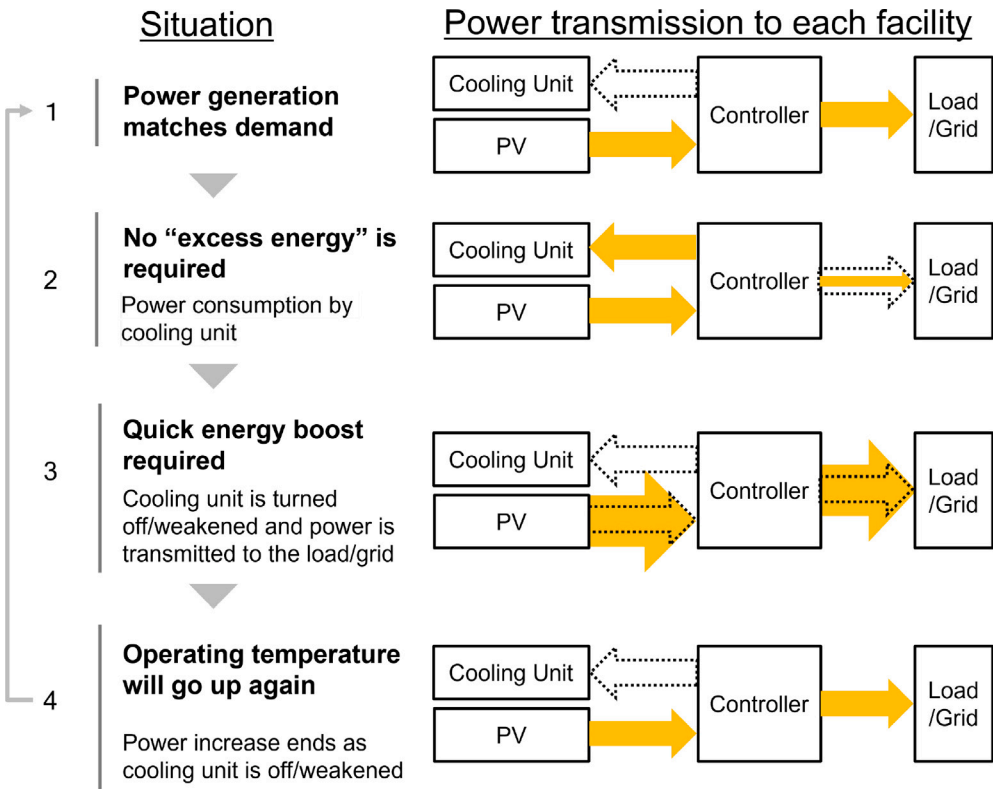

Fig. 3. Method of controlling power generation by PV cooling.

3.2. How to utilize PV cooling units

This section explains how the PV cooling unit, which is the key element of the proposed method, is used. Depending on the PV cell type, it has been shown that for every 1 °C increase in panel temperature, the maximum output of the PV cell decreases by 0.25% to 0.5% [25]. By integrating a cooling system, the proposed approach mitigates the negative effects of temperature rise on efficiency and ensures more stable output from the PV system. During PV output fluctuations, when output increases rapidly, the cooling unit is activated to consume excess power and cool the PV panels. On the other hand, if the output suddenly decreases, the cooling unit is deactivated or weakened, and the power is transmitted to the grid. This bidirectional coordination maintains a stable power supply to the grid and improves the efficiency and reliability of the entire power system. Energy injection into the cooling unit is not completely stopped or run, but is continuously adjusted up and down to bring the ramp rate closer to specification.

Fig. 3 shows a more concrete use of a PV cooling unit. In situation 1, PV generation matches demand or there are no significant fluctuations in PV output. In this state, the cooling unit does not operate. Next, in situation 2, when PV power generation becomes excessive due to increased solar irradiation, the cooling unit is activated to cool the panels along with the power consumed. This prevents power surges to the grid. Then, in situation 3, when a sudden increase in energy is required due to a sudden drop in solar irradiation or a sharp increase in demand, the cooling unit is turned off or weakened and the power is sent to the grid. Cooling allows PV panels with higher efficiency to generate more power at this time. This prevents a sudden drop in power to the load or the grid. In situation 4, the panel temperature gradually rises due to the stop of the cooling unit, and the power boost is terminated. This is considered long enough to prevent the ramp rate from rising due to PV output fluctuations. The specific operation plan for the PV cooling unit is established by solving an optimization problem based on the weather and load conditions at the time, as shown in Fig. 2.

4. Problem setting

This section provides the mathematical models introduced in the proposed method. It includes the microgrid model, the PV model, the PV cooling unit model, and the battery model, all of which are described in detail.

4.1. Targeted microgrids

The microgrid receives power from the main grid in the event of a power shortage. Whenever possible, excess power is either transmitted to the main grid, consumed by the PV cooling units and batteries, or wasted within the power plant. In general, the energy balance in the microgrid must thus be maintained at any given time t, which is formulated by:

$$S_t = P_t^{PV} + B_t^{out} - L_t - P_t^{cooling} - B_t^{in} - W_t, \quad \forall t, \tag{1}$$

where S_t is power transmitted/received, P_t^{PV} is PV generation, B_t^{out} is battery discharge, L_t is power load, $P_t^{cooling}$ is power consumed by the PV cooling unit, B_t^{in} is battery charge, and W_t is wasted power. The power transmitted/received S_t is positive when transmitted and negative when received. In addition, power consumed by the PV cooling unit $P_t^{cooling}$ and wasted power W_t cannot be negative, as given by Eqs. (2) and (3):

$$0 \le P_t^{cooling}, \quad \forall t, \tag{2}$$

$$0 \le W_t, \quad \forall t. \tag{3}$$

4.2. PV and PV cooling unit model

In this study, we utilized a mathematical PV-electrical model and an equivalent circuit-based PV-thermal model to estimate the electrical and the thermal constant time of the PV cell. Fig. 4 shows the illustration of the PV-electrical model, PV-thermal model, and PV cooling

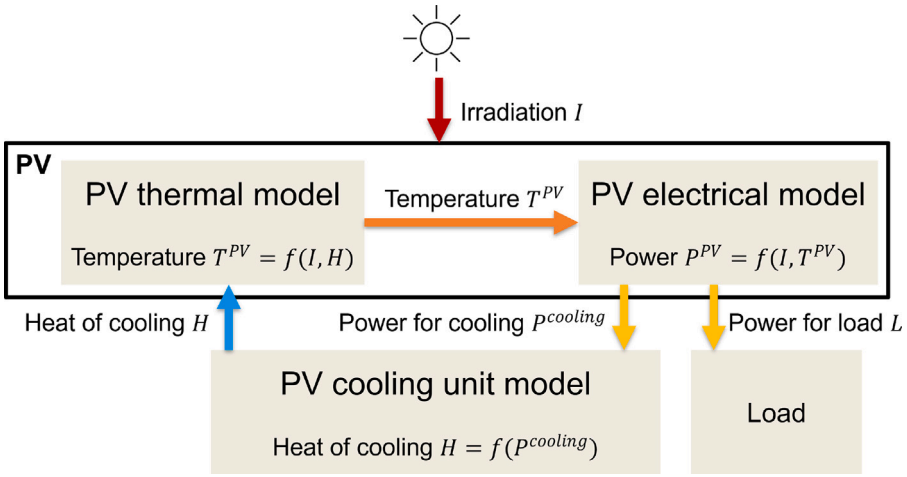

Fig. 4. PV-electrical, PV-thermal, and PV cooling unit model.

unit model used in this study and their input–output relationships. The PV-electrical and PV-thermal model is expressed by the following equations:

$$P_t^{PV} = \alpha \cdot (0.2047 \cdot I_t - 3.379) \cdot \{1.36464 - 0.36423 \cdot exp(0.00991 \cdot T_t^{PV})\} = \cdot \frac{1}{1000}, \quad \forall t, \tag{4}$$

$$T_{t+1}^{PV} = exp(-\frac{t}{\tau}) \cdot T_t^{PV} + \{1 - exp(-\frac{t}{\tau})\} \cdot T_t^{ambient} + R \cdot (-\frac{\alpha}{H_t} \cdot 1000 + I_t), \quad \forall t, \tag{5}$$

where α is number of panels, I_t is solar irradiation at time t, T_t^{PV} is PV panel temperature at time t, τ is the PV panel thermal constant time, $T_t^{ambient}$ is ambient temperature at time t, R is panel thermal resistance, H_t is heat produced by cooling unit at time t. The PV-electrical model was created by fitting data from real PV panel[1] which in charge of estimating PV power generation under different irradiation and temperature levels. The PV-thermal model was adapted from studies on energy management [32]. The panel temperature should not fall below a certain temperature, as given by Eq. (6), because the panel may not function if the panel temperature drops too low.

$$T^{PV,lower} \leq T_t^{PV}, \quad \forall t. \tag{6}$$

To simplify the modeling and optimization process, we utilized the simple coefficient of performance (COP) model for the PV cooling unit:

$$H_t = P_t^{cooling} \cdot COP, \quad \forall t, \tag{7}$$

where the H_t is calculated by an coefficient COP and power consumption of cooling unit $P_t^{cooling}$. For instance, the COP of single stage thermoelectric (peltier) cooler is typically between 0.3 to 0.7 and a typical air conditioner ranges from 5 to 8. Like the PV-thermal model, this model is also adapted from a study of online energy management for heating and cooling systems [33]. While we do not define specific cooling methods in this study, this model is suitable for most scenarios because it represents the ratio of energy consumed per unit time to energy cooled by the cooling units. In this study, we assume COP is a constant value for all environment condition.

4.3. Battery model

In this study, we use the simple internal resistance battery model [34] to estimate battery charge and discharge status. Fig. 5 shows the

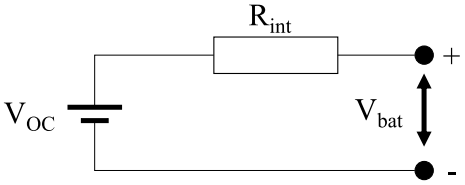

Fig. 5. Internal resistance battery model [34].

illustration of a typical internal resistance battery model, where the ideal open-circuit voltage source V_{OC} in series with an effective internal resistance R_{int}. The value of V_{OC} and R_{int} are vary from SOC.

The SOC of R_{int} model is estimated by coulomb counting method as shown in Eq. (8),

$$SOC = \frac{Ah_{rate} - Ah_{used}}{Ah_{rate}}, \tag{8}$$

with Ah_{rate} a rated maximum charge of the battery, and where

$$Ah_{used} = \int_0^t I(t)dt. \tag{9}$$

The change in the SOC level is calculated based on the battery current:

$$SOC_1 = SOC^{init}, \tag{10}$$

$$SOC_{t+1} = SOC_t + \frac{\gamma \cdot B_t^{in} - B_t^{out}}{B^{cap} \cdot 3600} \cdot \Delta t, \quad \forall t, \tag{11}$$

$$SOC^{min} \leq SOC_t \leq SOC^{max} \quad \forall t, \tag{12}$$

where γ is the charging efficiency, B^{cap} is the battery capacity, and Δt is the step length in the optimization calculation. In addition, the rates of charging and discharging are within a constant and they do not occur simultaneously, given by Eqs. (13), (14) and (15), respectively.

$$0 \leq B_t^{in} \leq C^{rate}, \quad \forall t, \tag{13}$$

$$0 \leq B_t^{out} \leq C^{rate}, \quad \forall t, \tag{14}$$

$$B_t^{in} \cdot B_t^{out} = 0, \quad \forall t, \tag{15}$$

where C^{rate} is the maximum charging/discharging power.

4.4. Mathematical formulation of PV system operation optimization

This section presents a detailed mathematical formulation of the scheduling of PV cooling unit and battery operation and power transfer to and from the main grid. The following formulation describes this scheduling optimization problem:

[1] Kyocera KC200GT.

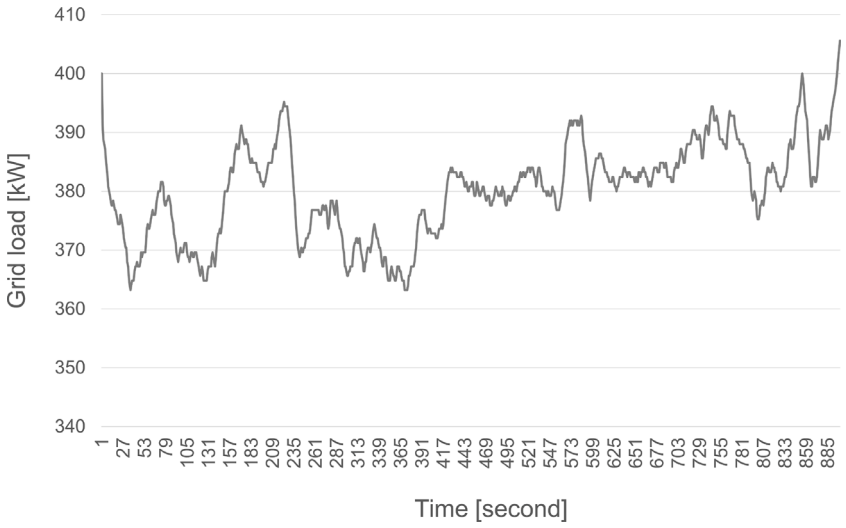

Fig. 6. Summer noon load data based on Oldenburg load frequency data. .

Table 2
Parameters settings of battery.

Description	Symbol	Value
Initial SOC	SOC^{init}	0.9
Min. SOC	SOC^{min}	0.2
Max. SOC	SOC^{max}	1.0
Max. charging/discharging power	C^{rate}	10 [kW]
Charging efficiency	γ	0.9

$$\text{minimize} \quad \sum_{t=1}^{l}(S_{t+1}-S_t)^2-\beta\sum_{t=1}^{l}S_t+\sum_{t=1}^{l}W_t, \tag{16}$$

subject to (1)–(15), $\forall t$,

input

$$\{L_t, I_t, T_t^{ambient}\},\ \forall t,$$

decision variables

$$\{S_t, P_t^{cooling}, B_t^{in}, B_t^{out}\},\ \forall\{t\},$$

where β is the coefficiency for scaling and l is the planning period. The objective function includes maximizing power to the main grid and minimizing wasted power, but the main objective is to minimize ramp rate. A nonlinear solver solves this optimization problem, and the solution involves optimal scheduling of PV cooling units, batteries, wasted power, and power transfer to and from the main grid.

5. Simulation results

In this section, we describe several key simulations to demonstrate the effectiveness of the proposed method under practical assumptions. The experimental setup is first described, followed by case studies. The effects of battery size and the coefficient of performance (COP), which represents the performance of the cooling unit, on ramp rate control performance are also discussed.

5.1. Simulation setup

The parameters of the proposed method are presented here. For all simulations, the simulation period is 15 min and the time resolution is 1 s. β in Eq. (16) was set to the constant value of 0.0000982. The battery parameters in the optimization problem are listed in Table 2. These battery parameters are set with reference to previous studies of energy management using batteries [32]. Outdoor temperature and solar irradiation data for Oldenburg were collected with a resolution of 1 s. As shown in Fig. 7, the data covers a 15-min period during which PV generation is highly variable. The 15 min selected for simulation for each season and time period are shown in Table 3. The morning is selected two hours after sunrise of each day and the evening is selected two hours before sunset of each day. The parameters related to PV in the optimization problem are listed in Table 4. The number of PV panels is set to simulate a PV plant with a maximum output of 1 MW. PV panel thermal resistance and PV panel thermal constant time are set with reference to the previous study on PV panels [35]. The load profiles were created based on the actual grid frequency data for Oldenburg. The base components of the load profiles were set as shown in Table 5 for each season and time of day according to the size of the PV plant assumed in this study. The noise component created from the Oldenburg grid frequency data combined with this fundamental component is shown in Fig. 6. This load data is used as input for the simulation. The evaluation metric, ramp rate, is defined by:

$$Ramp\ rate = \frac{|\Delta P|\cdot T_s}{timescale}, \tag{17}$$

where ΔP describes the change in power S_t, i.e., $\Delta P = |S_{t+1} - S_t|$, exchanged between the microgrid and the main grid, T_s describes data resolution ($T_s = 1$ in this study), $timescale$ describes the time scale for calculating ramp rate ($timescale = 1$ in this study).

5.2. Impact of PV cooling on ramp rate

In this section, we examine the effect of PV cooling on ramp rates. This simulation was performed for each season and time period. In this simulation, the battery capacity was set to 10 kWh and the COP of the cooling unit to 15.

Focusing on summer noon (July 7, 12:30-12:45) when solar irradiation is high, Table 6 shows the mean ramp rate and maximum ramp rate with and without PV cooling. From Table 6, it can be seen that both the mean ramp rate and the maximum ramp rate decreased with PV cooling. Specifically, the mean ramp rate decreased by 43.5% and the maximum ramp rate decreased by 76.2%.

To see how this could be accomplished, Fig. 8 shows the simulation results for 200 s during the 15-min period of the simulation, when solar irradiation changed significantly. Fig. 8(a) shows how power is used. In Fig. 8(b), the ambient and panel temperatures and solar irradiation are shown. The dotted line is for the case without cooling. The horizontal axis is common in Fig. 8(a) and (b). Comparing the power with the grid with and without cooling in Fig. 8(a), we see that the change in power, or ramp rate, is smaller with cooling than without cooling. First, around 375 s, the solar irradiation shown in brown in Fig. 8(b) begins

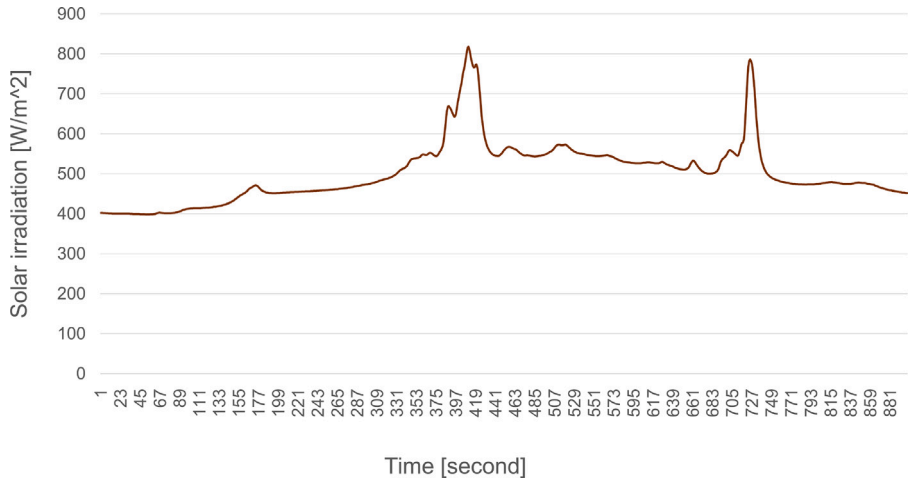

Fig. 7. Solar irradiation in Oldenburg on July 7, 2015 from 12:30 to 12:45.

Table 3
Date and time of selected 15 min of temperature and solar irradiation data for each season and time of day.

Season	Time of day		
	Morning	Noon	Evening
Autumn	October 7, 2014 9:30–9:45	October 7, 2014 12:00–12:15	October 7, 2014 16:00–16:15
Winter	January 7, 2015 10:45–11:00	January 7, 2015 12:30–12:45	January 7, 2015 14:00–14:15
Spring	April 7, 2015 10:00–10:15	April 7, 2015 12:00–12:15	April 7, 2015 16:45–17:00
Summer	July 7, 2015 7:30–7:45	July 7, 2015 12:30–12:45	July 7, 2015 18:45-19:00

Table 4
Parameters settings of PV.

Description	Symbol	Value
Lower temperature limit of PV panel	T^{lower}	10 [°C][a]
Nominal solar irradiation	$I^{nominal}$	800 [W/m^2]
PV panel thermal resistance	R	0.01874 [K/W]
Number of PV panels	α	5000
PV panel thermal constant time	τ	1128 [s]

[a] When PV panel temperature is originally less than 10 °C, T^{lower} is 0.

Table 5
Base components of load profiles by season and time of day [kW].

Season	Time of day		
	Morning	Noon	Evening
Autumn	20	400	20
Winter	500	400	60
Spring	300	400	40
Summer	500	400	60

Table 6
Mean and maximum ramp rates with and without cooling during the summer noon.

Valuation index	w/o cooling	w/ cooling
Mean ramp rate [kW/s]	0.6850	0.3871
Maximum ramp rate [kW/s]	8.111	1.929

to increase rapidly. Then, the amount of power generation shown in Fig. 8(a) also increases due to the increase in solar irradiation. Since the ramp rate will increase at this rate, the cooling unit operates as shown in light blue to cool the PV panels at the same time that power is consumed. This reduces the surge of power to the grid, as can be seen in Fig. 8(a). The pre-cooling of the PV also prevents an increase in ramp rate due to the sudden decrease in solar irradiation. Fig. 8(b) shows a sharp decrease in solar irradiation, indicated in brown, around 420 s. The decrease in solar irradiation reduces the power generation as shown in Fig. 8(a), but because of the pre-cooling, the decrease is less than in the case without cooling, shown by the dotted line. In addition to that, by gradually weakening the cooling unit and sending the power consumed by the unit to the grid, the change in power to the grid is smoother in the solid line with cooling, as shown in Fig. 9, a partially enlarged version of Fig. 8.

Fig. 10 shows the mean and maximum ramp rates for each season and time period. Since there are large differences in solar irradiation and variations in ramp rates by season and time of day, the values are shown relative to the case without cooling at each season and time of day, with 1 being the case without cooling. Fig. 10 shows that the ramp rate reduction rate of the proposed method is achieved regardless of season or time of day. Reductions are greater in the morning, evening, and winter months, which is thought to be due to the relative ease of ramp rate reduction because the ramp rate during these times and seasons is relatively small.

5.3. Impact of battery size and cooling unit COP

In this section, we investigate how varying the battery capacity and the COP, which represents the performance of the cooling unit, affects the ramp rate. The battery capacities evaluated are 0 (no battery), 10, 20, 30, 40, 70, and 100. The COPs of the cooling units evaluated are 1, 3, 5, 10, and 15. This simulation is performed using data from 15 min of summer noon (12:30–12:45 on July 7, 2015). Using a cooling unit with a small COP may reduce the ramp rate only by consuming power, without improving the efficiency of power generation through cooling. Since this is not desirable, we added, in addition to ramp rate as an evaluation metric, the accumulated energy, which is the accumulated amount of energy sent from the microgrid to the main grid (i.e., equals $\sum_{t=1}^{l} S_t$, with l still the planning period). This value is typically smaller if the cooling unit does not improve the efficiency of power generation by the PV panels.

The mean ramp rate (a), maximum ramp rate (b), and accumulated energy (c) at each battery capacity and COP are shown in Fig. 11. The horizontal axis is commonly the battery capacity, and the dotted line shows the results without cooling. Fig. 11(a) and (b) show that for all battery capacities and COPs, the mean and maximum ramp rates are smaller with cooling than without cooling. Focusing on the part of the

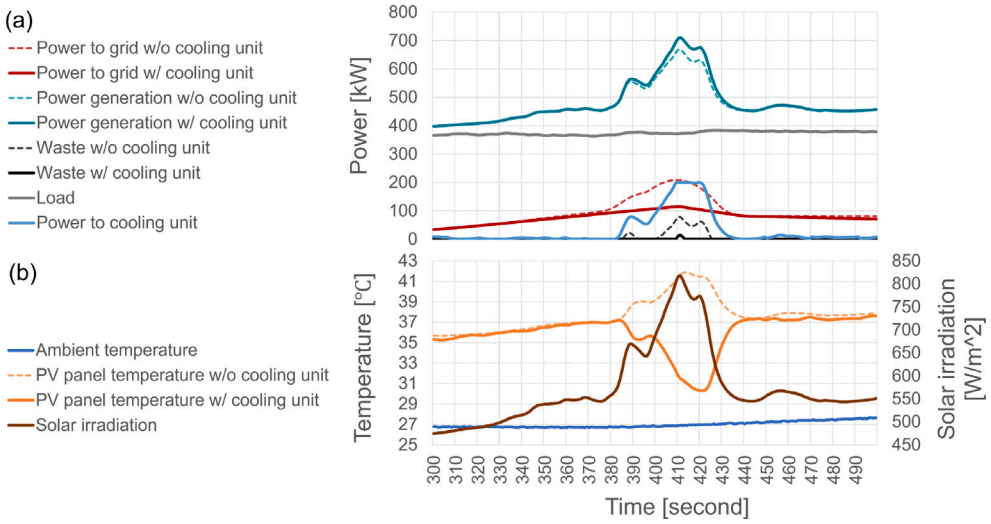

Fig. 8. Changes in power (a) and temperature (b) during the 200 s of summer noon when the solar irradiation changed significantly.

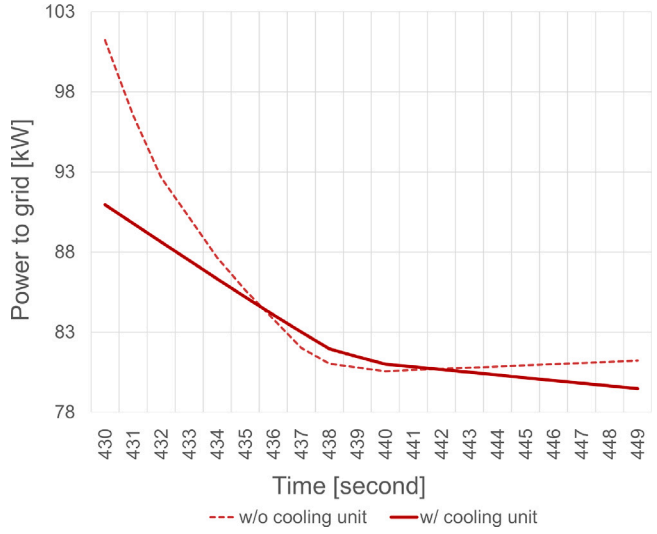

Fig. 9. Power to the grid, with and without cooling, between 430 and 450 s.

battery capacity up to 40 kWh, a ramp rate reduction of more than 50% compared to without cooling is achieved with a maximum loss of only about 10 kWh of accumulated energy. Even a really easy value to achieve, COP = 1, provides very good ramp rate control, although it reduces the amount of power transmitted to the grid. Focusing on the part of the battery capacity above 70 kWh, while there is more loss of accumulated energy than without cooling from Fig. 11(c), the mean and maximum ramp rates are almost zero from Fig. 11(a) and (b). These results indicate that lower COP values contribute significantly to ramp rate control despite lower energy efficiency, highlighting the robustness of this method to fluctuations in cooling unit performance. The potential cost savings and environmental benefits are highlighted by the ability to effectively manage ramp rate variability when combined with effective PV cooling, even with small battery capacities. Finally, the battery capacities required to achieve the same ramp rate are compared. Fig. 11(a) and (b) show that the mean and maximum ramp rate that can be achieved with a 20 kWh battery with cooling would require, although somewhat different depending on COP, nearly 100 kWh of battery to achieve without cooling. In other words, the proposed method reduced the required battery capacity by nearly 80%.

6. Summary

We propose a ramp rate control method using PV cooling for PV systems. The proposed method controls the power supply to the grid by power consumption and increases the efficiency of power generation by PV cooling units, without using large-capacity batteries or gas turbines, which have a high environmental impact and system cost. Compared to the ramp rate control method that only uses batteries without PV cooling, the results demonstrate that the proposed method can reduce the maximum ramp rate by up to 76. 2% during summer noon. The impact of battery capacity and PV cooling unit COP on the performance of the proposed method was also investigated. It was found that not only the cooling unit alone can reduce the ramp rate, but also the combination of a small-capacity battery can significantly reduce ramp rate with little energy loss. Finally, we clarify the assumptions, restrictions and possible remedies.

- **Expansion of test scenarios**: Current simulations are based on specific meteorological data. To further validate the robustness of the proposed approach, it is planned to test the approach over a wider range of geographic locations and weather conditions. It could also be applied to small-scale testbed studies to demonstrate the feasibility of the approach.
- **Cooling technology selection**: The challenges associated with the practical deployment of cooling technologies must be addressed by optimizing the technology not only for performance and reliability but also for cost-effectiveness. Future research will include the selection of cooling technologies that incorporate performance and the cost of integration, operation, and maintenance as key factors.
- **Economic feasibility**: Although we highlighted the environmental and cost benefits compared to systems involving large-capacity batteries or gas turbines, before proceeding to a product prototype, a more comprehensive economic analysis would be needed. Future work will include a detailed cost–benefit analysis, including life-cycle costs, to better understand the economic feasibility of the proposed approach.
- **Convexification of the optimization model**: Since the optimization problem is nonlinear programming, the result obtained is one optimal solution, but better solutions may exist. Methods to convert current nonlinear optimization problems to convex form can be explored. This transformation could guarantee optimality of the solution, improve computational efficiency, and make real-time applications more realistic on limited platforms.

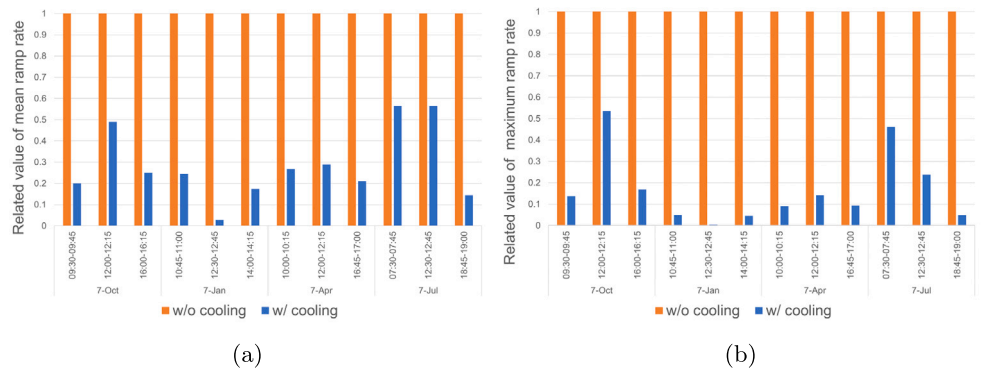

Fig. 10. Mean ramp rate (a) and maximum ramp rate (b) for each season and time period relative to 1 for without cooling.

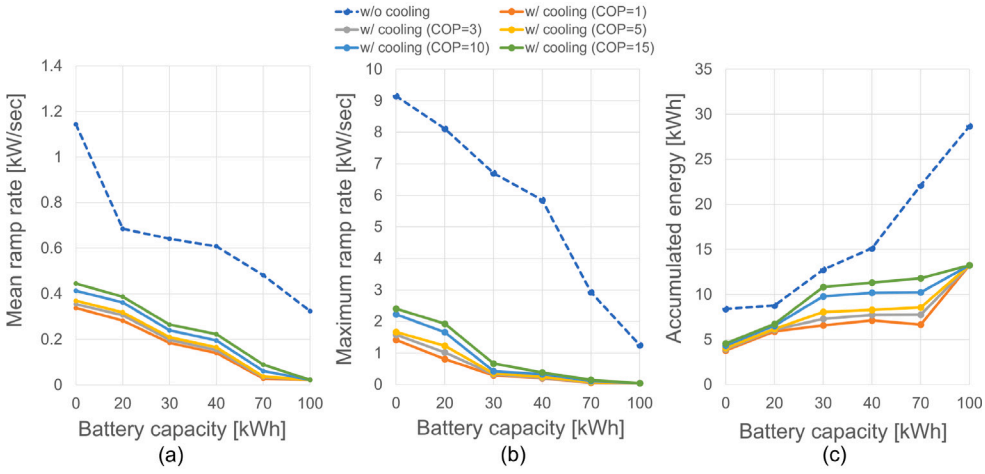

Fig. 11. Mean ramp rate (a), maximum ramp rate (b), accumulated energy (c) at each battery capacity and COP.

- **Validation in Residential Applications**: While the application of our ramp rate control method to residential settings has potential benefits such as increased energy self-sufficiency and enhanced grid stability, there are also practical challenges such as system sizing, local regulations, heterogeneous household energy use patterns, and limited space for PV panels and cooling equipment. Part of future research includes an empirical examination of the effectiveness of ramp rate control methods in residential settings. This includes examining how the proposed method can be adapted to manage the unique needs and constraints of residential environments.

CRediT authorship contribution statement

Koki Iwabuchi: Writing – original draft, Visualization, Validation, Software, Methodology, Investigation, Formal analysis, Conceptualization. **Daichi Watari:** Software, Methodology. **Dafang Zhao:** Writing – original draft, Visualization, Software, Methodology, Investigation, Formal analysis. **Ittetsu Taniguchi:** Supervision, Investigation. **Francky Catthoor:** Writing – review & editing, Supervision, Project administration, Methodology, Conceptualization. **Takao Onoye:** Supervision.

Declaration of competing interest

The authors declare that they have no known competing financial interests or personal relationships that could have appeared to influence the work reported in this paper.

Acknowledgments

The authors would like to express our sincere gratitude to colleagues from NTUAthens, AUTH and IMEC for the valuable discussions and insights, which significantly contributed to the development of this research.

Data availability

The authors do not have permission to share data.

References

[1] Amorim WCS, Cupertino AF, Pereira HA, Mendes VF. On sizing of battery energy storage systems for PV plants power smoothing. Electr Power Syst Res 2024;229:110114. http://dx.doi.org/10.1016/j.epsr.2024.110114.

[2] Abudu K, Igie U, Minervino O, Hamilton R. Gas turbine efficiency and ramp rate improvement through compressed air injection. Proc Inst Mech Eng A 2021;235(4):866–84.

[3] Omran WA, Kazerani M, Salama MMA. Investigation of methods for reduction of power fluctuations generated from large grid-connected photovoltaic systems. IEEE Trans Energy Convers 2011;26(1):318–27. http://dx.doi.org/10.1109/TEC.2010.2062515.

[4] Ali HM, Mahmood M, Bashir MA, Ali M, Siddiqui AM. Outdoor testing of photovoltaic modules during summer in Taxila, Pakistan. Therm Sci 2016;20(1):165–73.

[5] Ali HM. Recent advancements in PV cooling and efficiency enhancement integrating phase change materials based systems – A comprehensive review. Sol Energy 2020;197:163–98. http://dx.doi.org/10.1016/j.solener.2019.11.075.

[6] Lappalainen K, Valkealahti S. Sizing of energy storage systems for ramp rate control of photovoltaic strings. Renew Energy 2022;196:1366–75.
[7] Martins J, Spataru S, Sera D, Stroe D-I, Lashab A. Comparative study of ramp-rate control algorithms for PV with energy storage systems. Energies 2019;12(7). http://dx.doi.org/10.3390/en12071342.
[8] Beltran H, Tomás García I, Alfonso-Gil JC, Pérez E. Levelized cost of storage for li-ion batteries used in PV power plants for ramp-rate control. IEEE Trans Energy Convers 2019;34(1):554–61. http://dx.doi.org/10.1109/TEC.2019.2891851.
[9] Abdelghany MB, Al-Durra A, Gao F. A coordinated optimal operation of a grid-connected wind-solar microgrid incorporating hybrid energy storage management systems. IEEE Trans Sustain Energy 2024;15(1):39–51. http://dx.doi.org/10.1109/TSTE.2023.3263540.
[10] Gonzalez-Moreno A, Marcos J, de la Parra I, Marroyo L. A PV ramp-rate control strategy to extend battery lifespan using forecasting. Appl Energy 2022;323:119546.
[11] Atif A, Khalid M. Saviztky–golay filtering for solar power smoothing and ramp rate reduction based on controlled battery energy storage. IEEE Access 2020;8:33806–17.
[12] Jiménez E, Madrigal M. Mitigation of PV power fluctuations using moving average control in an openDSS-python environment. In: 2020 IEEE international autumn meeting on power, electronics and computing. ROPEC, Vol. 4, 2020, p. 1–6. http://dx.doi.org/10.1109/ROPEC50909.2020.9258771.
[13] Alvaro D, Arranz R, Aguado JA. Sizing and operation of hybrid energy storage systems to perform ramp-rate control in PV power plants. Int J Electr Power Energy Syst 2019;107:589–96.
[14] Arévalo P, Benavides D, Tostado-Véliz M, Aguado JA, Jurado F. Smart monitoring method for photovoltaic systems and failure control based on power smoothing techniques. Renew Energy 2023;205:366–83.
[15] Benavides D, Arévalo P, Tostado-Véliz M, Vera D, Escamez A, Aguado JA, Jurado F. An experimental study of power smoothing methods to reduce renewable sources fluctuations using supercapacitors and lithium-ion batteries. Batteries 2022;8(11):228.
[16] Abdelghany MB, Al-Durra A, Daming Z, Gao F. Optimal multi-layer economical schedule for coordinated multiple mode operation of wind-solar microgrids with hybrid energy storage systems. J Power Sources 2024;591:233844. http://dx.doi.org/10.1016/j.jpowsour.2023.233844.
[17] Lim YS, Tang JH. Experimental study on flicker emissions by photovoltaic systems on highly cloudy region: A case study in Malaysia. Renew Energy 2014;64:61–70. http://dx.doi.org/10.1016/j.renene.2013.10.043.
[18] Shivashankar S, Mekhilef S, Mokhlis H, Karimi M. Mitigating methods of power fluctuation of photovoltaic (PV) sources–a review. Renew Sustain Energy Rev 2016;59:1170–84.
[19] Tonkoski R, Lopes LA, El-Fouly TH. Coordinated active power curtailment of grid connected PV inverters for overvoltage prevention. IEEE Trans Sustain Energy 2010;2(2):139–47.
[20] Rostami S, Afrand M, Shahsavar A, Sheikholeslami M, Kalbasi R, Aghakhani S, Shadloo MS, Oztop HF. A review of melting and freezing processes of PCM/nano-PCM and their application in energy storage. Energy 2020;211:118698.
[21] Siahkamari L, Rahimi M, Azimi N, Banibayat M. Experimental investigation on using a novel phase change material (PCM) in micro structure photovoltaic cooling system. Int Commun Heat Mass Transfer 2019;100:60–6.
[22] Abdollahi N, Rahimi M. Potential of water natural circulation coupled with nano-enhanced PCM for PV module cooling. Renew Energy 2020;147:302–9.
[23] Madurai Elavarasan R, Nadarajah M, Pugazhendhi R, Gangatharan S. An experimental investigation on coalescing the potentiality of PCM, fins and water to achieve sturdy cooling effect on PV panels. Appl Energy 2024;356:122371. http://dx.doi.org/10.1016/j.apenergy.2023.122371.
[24] Mehrali M, ten Elshof JE, Shahi M, Mahmoudi A. Simultaneous solar-thermal energy harvesting and storage via shape stabilized salt hydrate phase change material. Chem Eng J 2021;405:126624.
[25] Hamzat AK, Sahin AZ, Omisanya MI, Alhems LM. Advances in PV and PVT cooling technologies: A review. Sustain Energy Technol Assess 2021;47:101360. http://dx.doi.org/10.1016/j.seta.2021.101360.
[26] Selimefendigil F, Şirin C. Energy and exergy analysis of a hybrid photovoltaic/thermal-air collector modified with nano-enhanced latent heat thermal energy storage unit. J Energy Storage 2022;45:103467.
[27] Wang W, Aleid S, Shi Y, Zhang C, Li R, Wu M, Zhuo S, Wang P. Integrated solar-driven PV cooling and seawater desalination with zero liquid discharge. Joule 2021;5(7):1873–87.
[28] Mahdavi A, Farhadi M, Gorji-Bandpy M, Mahmoudi A. A comprehensive study on passive cooling of a PV device using PCM and various fin configurations: Pin, spring, and Y-shaped fins. Appl Therm Eng 2024;252:123519. http://dx.doi.org/10.1016/j.applthermaleng.2024.123519.
[29] Bayrak F, Oztop HF, Selimefendigil F. Experimental study for the application of different cooling techniques in photovoltaic (PV) panels. Energy Convers Manage 2020;212:112789.
[30] Li R, Shi Y, Wu M, Hong S, Wang P. Photovoltaic panel cooling by atmospheric water sorption–evaporation cycle. Nat Sustain 2020;3(8):636–43.
[31] Dwivedi P, Sudhakar K, Soni A, Solomin E, Kirpichnikova I. Advanced cooling techniques of p.v. modules: A state of art. Case Stud Therm Eng 2020;21:100674. http://dx.doi.org/10.1016/j.csite.2020.100674.
[32] Watari D, Taniguchi I, Goverde H, Manganiello P, Shirazi E, Catthoor F, Onoye T. Multi-time scale energy management framework for smart PV systems mixing fast and slow dynamics. Appl Energy 2021;289:116671. http://dx.doi.org/10.1016/j.apenergy.2021.116671.
[33] Zhao D, Watari D, Ozawa Y, Taniguchi I, Suzuki T, Shimoda Y, Onoye T. A thermal comfort and peak power demand aware VRF heating/cooling management framework: Simulation and on-site experiment. J Inf Process 2022;30:476–85. http://dx.doi.org/10.2197/ipsjjip.30.476.
[34] Johnson V. Battery performance models in ADVISOR. J Power Sources 2002;110(2):321–9. http://dx.doi.org/10.1016/S0378-7753(02)00194-5.
[35] Kurz D, Nawrowski R. Thermal time constant of PV roof tiles working under different conditions. Appl Sci 2019;9(8). http://dx.doi.org/10.3390/app9081626.